Journal of the Korean Magnetic Resonance Society **2009**, *13*,143-153

NMR Studies of Ni-binding Luteinizing Hormone Releasing Hormone

Jin Kim and Hoshik Won*

*Department of Applied Chemistry, Hanyang University, Sa3-Dong 1271, Ansan, Kyunggi-Do, Korea

Abstract : Luteinizing Hormone Releasing Hormone (LHRH) is composed of 10 amino acids, and is best known as a neurotransmitter. Because of the 80% homology in animals, much more concerns have focused on the substances that have similar functions or can control LHRH. Ni,Cu-LHRH complexes were synthesized. The degree of complexation was monitored by ^{1}H, ^{13}C-NMR chemical shifts, and final products were identified by ESI-Mass spectrum. Solution-state structure determination of Ni-LHRH complex was accomplished by using NMR results and NMR-based distance geometry (DG). Interproton distances from nuclear Overhauser effect spectroscopy (NOESY) were utilized for the molecular structure determination. Results were compared with previous structures obtained from energy minimization and other spectroscopic methods. Structure obtained in this study has a cyclic conformation which is similar to that of energy minimized, and exhibits a specific α-helical turn with residue numbers (2~7) out of 10 amino acids. Comparison of chemical shifts and EPR studies of Ni,Cu-LHRH complexes exhibit that Ni-LHRH complex has same binding sites with the 4-coordination mode as in Zn-LHRH complex.

Keywords : NMR, EPR, Ni- LHRH Complex, Solution state structure

INTRODUCTION

Luteinizing hormone-releasing hormone (LHRH, or GnRH = gonadotropin- releasing hormone, MW=1,182) is a decapeptide endocrine biomolecule which regulates of the secretion of gonadotrophins, luteinizing hormone (LH), and the follicle stimulating hormone (FSH). The LHRH, best known as a main neurotransmitter, has following a amino acid sequence pGlu[1]-His[2]-Trp[3]-Ser[4]-Tyr[5]-Gly[6]-Leu[7]- Arg[8]-Pro[9]-Gly[10]-

* To whom correspondence should be addressed. E-mail : hswon@hanyang.ac.kr

NH_2. The synthesis and release of this peptide is regulated by the central nervous system and subject to environmental influences such as age, light, olfactory stimuli, and sexual stimulation [1~3].

Although numerous LHRH analogs have been synthesized and structurally characterized, relatively little is known about the processes by which the LHRH receptor is activated during the hormone action [4-13]. For agonist and antagonist synthesis, the substitution with L-amino acids on the position of Gly[6] decreases activities, whereas the substitution with D-amino acids (D-Ala, D-Val) increases the activity much more than that of native LHRH [14~16]. The properties of dimeric analogs (D-Gly10-[D-Lys6]GnRH-NHEt) indicate that the LHRH receptor is more readily activated by a bivalent ligands. Several antagonists were synthesized by using solid phase peptide synthetic method to test receptor binding on the basis of some cyclic peptide analogs of LHRH. The most potent cyclic peptide antagonist analog is known as Ac-D-Phe(p-Cl)-D-Trp-Ser-Glu-D-Arg -Leu-Lys-Pro-D-ala-NH_2. Energy minimization methods and molecular dynamic studies [18~20] show that this cyclic antagonist analog has a modified ß-bend between residue position [5] and [8].

Since Burrows [21] showed that the chelated copper is a highly potent and possibly endogenous agent which includes the release of LHRH from its neurosecretary cells in the hypothalamus, the metal-binding effect of LHRH has been reevaluated in physiological pathway because of their structurally unique function. The copper, chelated to putative circulating chelators, markedly stimulates LHRH release. Focusing on the stimuli of metal chelator and on the release of LHRH from the hypothalamus into the portal blood, there have been many papers published to discuss various aspects of conformational dynamics and metal binding effects of LHRH. Although lot of LHRH analogs have been synthesized and theoretically studied, detailed mechanistic roles and functions are not known for the free LHRH and metal-binding complexes of LHRH.

Although dose-response experiments (physiological test) provide information on the efficiency of LHRH analogs, it does not give any detailed structural features, including a mechanism of LHRH releasing and the coordination chemistry of metal-binding LHRH which may provide important features of therapeutic agents. The purpose of this paper is to understand the transition metal-dependent regulation of LHRH releasing from hyperthalamus as well as the coordination chemistry of metal-binding LHRH (or affinities

of metal chelators to LHRH) in stimulated LHRH releasing process. Structural characterization by using NMR and NMR-based Distance Geometry (DG) were carried out to obtain further insights of the stimulated LHRH releasing process.

EXPERIMENTALS

Reagent

Neurohormone LHRH(purity 99%) were purchased from Sigma, and atomic absorption standard solution of metal ions including $NiCl_2$, $CuCl_2$ were purchased from Aldrich. LHRH was dessolved in demineralized HPLC grade pure water (pH 5.3), and subsequently standard metal ion were added for complexation. During the complexation, the pH of each sample adjusted to pH 6.5 ~6.8 by titration of 0.001M NaOH and HCl pertinently. The degree of complexation was monitored by NMR chemical shift change, and the final mass of each complex was identified with ESI-Mass. After drying this solution by freeze dryer, sample was solved in D_2O/H_2O solvent for NMR experiments.

NMR Experiments

NMR sample was prepared by dissolving 10 mg of synthetic peptide into 500 mL of D_2O and H_2O. All NMR data were collected on Varian 500 MHz and 300 MHz system at 25 ℃ by using homonuclear and heteronuclear correlation experiments including correlation spectroscopy (COSY), total correlation spectroscopy (TOCSY), nuclear Overhauser effect spectroscopy (NOESY), HMQC, and HMBC techniques. COSY : 2x256x1024 raw data matrix size; 16 scans per t1 increment; 1.5 s repetition delay; 6 Hz Gaussian and 90° shifted squared sine bell filtering in the t2 and t1 domains, respectively. TOCSY : 2x256x1024 raw data matrix size; 32 scans per t1 increment; 1.5 s repetition delay; 65 ms MLEV-16 continuous wave spin lock period; 6.25 kHz spin lock field strength, corresponding to 42μs 90° pulse width; 6 Hz Gaussian and 90° shifted squared sine bell filtering in the t2 and t1 domains, respectively. NOESY : 2x256x1024 raw data matrix size; 64 scans per t1 increment; 2.8 s repetition delay period; 10, 50, 100, 300, 500 ms mixing period for nuclear Overhauser effect (NOE) buildup profile; 6 Hz Gaussian and 90° shifted

squared sine bell filtering in the t2 and t1 domains, respectively. HMQC : 2x128x1024 raw data matrix size; 128 scans per t1 increment; 1.2 s repetition delay; 33 μs 90° ^{13}C pulse widths; 16W RF broad band Walts-16 ^{13}C decoupling during acquisition period; 3.5 ms defocusing and refocusing delay periods; 800ms "Weft" period; 6Hz Gaussian and 90° shifted squared sine bell filtering in the t2 and t1 domains, respectively. HMBC : 2x128x1024 raw data matrix size; 512 scans per t1 increment; 2.0 s repetition delay period; 33 μs 90° ^{13}C pulse widths; 3.5 ms delay period for suppression of one-bond signals; 40 ms delay periods for long-range coupling; 15° shifted sine-bell filtering in the t2 domain, and no filtering in the t1 domain.

NMR Signal Assignment and Structure Determination

Complete ^{1}H-NMR signal assignments of metal free LHRH and Ni-binding LHRH were accomplished by 2D COSY, TOCSY, NOESY experiments [22-23] . The degree of zinc complexation was made by micro titration. Spectral comparisons were made for the spectral region of alpha proton and NH proton. The changes of chemical shift provide the possible metal binding site and structural information (Fig. 1 and Fig. 2). ^{1}H-NMR signal assignments were made by determining scalar connectivities within amino acid residues from COSY spectrum and then correlating the signals of adjacent residues on the basis of dipolar connectivities obtained from 2D NOESY data.(Table 1)

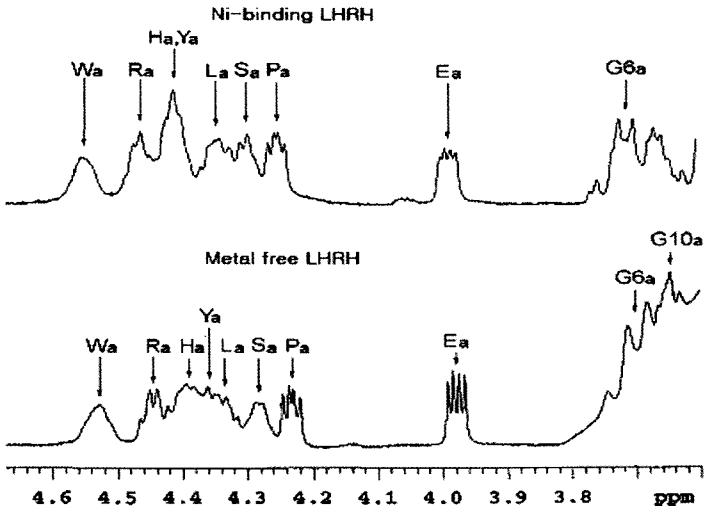

Fig. 1. The spectral region of alpha protons of peptide bonds and aromatic protons are shown for LHRH and Ni-binding LHRH

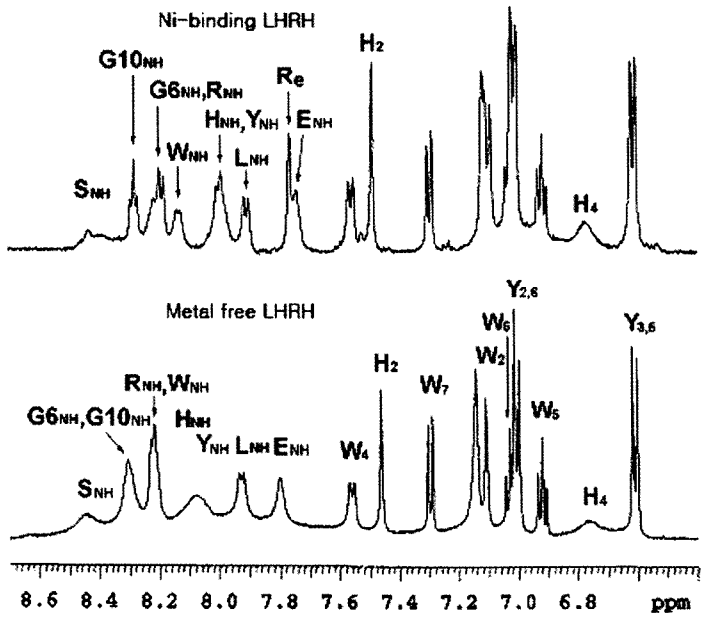

Fig. 2. The spectral region of NH protons of peptide bonds and aromatic protons are shown for LHRH and Ni-binding LHRH

Table 1. Important NOE connectivities used for the structure determination of Ni-binding LHRH.*

H Signals	Chemical Shift (ppm)	NOE Connectivities
W(NH)	8.12	Wa(s), Wß(vw)
G10(NH)	8.30	Pa(s), G10a(s)
G6(NH)	8.21	G6a(s), Yß(w)
R(NH)	8.20	Ra(s), Rß(m), Lß(m), La(s)
H(NH)	8.03	Wa(w), Ha(s), Ea(w), Wß(w), Hß(w)
Y(NH)	7.09	Wa(m)
S(NH)	8.42	Wa(w), Ya(m), Sa(s), G6a(vw), Tß(m)
L(NH)	7.82	La(m), G6a(s), Lßr(s), Lßs(m), G6(NH)(m)
E(NH)	7.75	Ea(m)
W4	7.57	Wa(w), Wß(w)
W7	7.57	Wa(w), Wß(w)
W6	7.14	Wa(w), Wß(w)
Y2	7.03	Ya(w), Yß(m), Y3(s)
Y6	7.03	Ya(w), Yß(m), Y5(s)
H4	6.83	Hß(w), Ha(vw)
La	4.35	Lß (m)
Y2,6	7.02	W2,5(m), Y3.5(s), W(NH,ring)(m)
W2,5	7.04	W(NH,ring)(w), W4,7(s)
H(NH,ring)	10.9	W(NH,ring)(m), G10(NH_2)(m), W6(s), W(NH)(vw)

*NOEs are classified into strong(s), medium(m), weak(w), very weak(vw) based on intensity. Prociral assignment were used for methylene proton as *r* and *s*, respectively. Positions of each proton are labeled with Ca (a) and Cß(ß) and numbering scheme for functional group.

Molecular geometry associated with electronic structures of Ni,Cu-LHRH complexes exhibiting paramagnetic properties gave rise to signal broadening and change of chemical shifts near binding sites. X-band EPR spectrum of Ni,Cu-LHRH complexes exhibit that complexes have same binding sites with the 4-coordination as in Zn-LHRH complex. The EPR spectrum of Ni,Cu-LHRH with $g_{\parallel}$=2.207, $g_{\perp}$= 2.067, $a_{\parallel}$=192.383 are shown in Fig. 3.

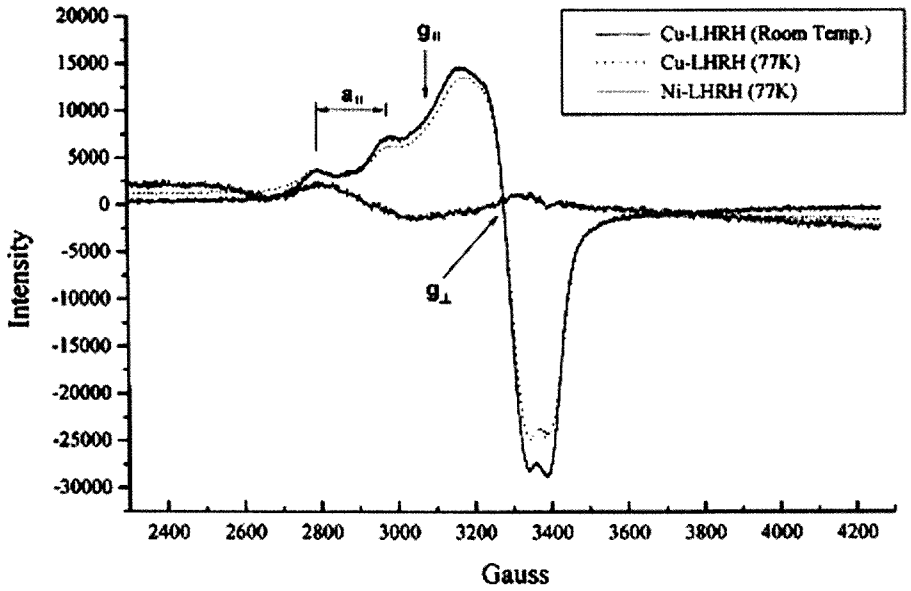

Fig. 3. EPR studies of Ni,Cu-LHRH complexes exhibit that they have same binding sites with the 4-coordination Zn-LHRH complex. X-band EPER spectrum of Ni,Cu-LHRH complexes with $g_{\parallel}$=2.207, $g_{\perp}$= 2.067, $a_{\parallel}$=192.383 values were observed.

Structure determinations were carried out using HYGEOM^{TM}, HYNMR^{TM} [24] . In structural interpretations with distance geometry the experimental NOE constraints are best interpreted as a range of equally probable values for the distances in question. NOE restraints were divided into cross peaks classified as strong, medium, weak and very weak. The ranges of NOE restraints were assigned with 2.0-2.9(strong peaks), 2.0-3.5(medium

peaks), 3.5-4.5(weak peaks), 3.5-5.0(very weak peaks). Standard pseudo atom corrections were applied to the NOE restraints. Distance geometry (DG) structures were generated and refined by using primary restraints. Trial distances generated by selecting random distances between the upper and lower bounds of each element were embedded (Fig. 4). These DG structures were then subjected to conjugate gradient minimization (CGM), affording new structures with penalties in the range of ca. 0.8-2.0Å^2. When additional CGM was unable to further reduce the penalty for a particular structure.

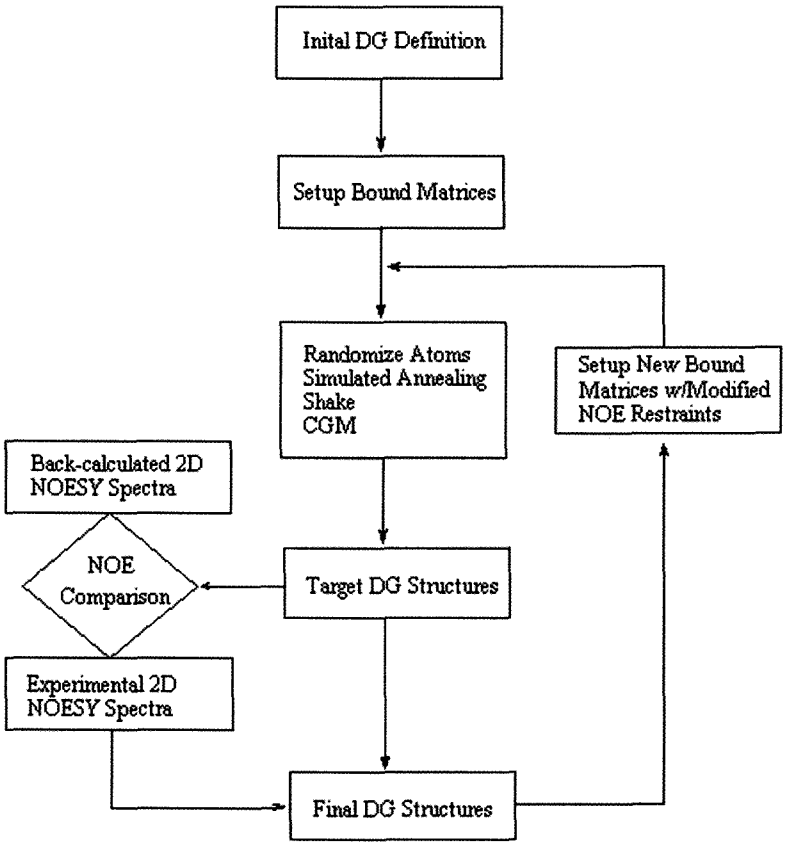

Fig. 4. Flow diagram used for the NMR-based distance geometry computation

2D NOESY back calculations were performed, and new distance restraints dictated by discrepancies between the experimental and back-calculated spectra were added to the

experimental restraint list. Freshly embedded DG structures minimized with the modified restraints list generally exhibited penalty values lower than those of the previously refined structures and the new DG structures generally gave back-calculated NOESY spectra that were more consistent with experimental data. This cycle of (1) random embedding, (2) minimal simulated annealing and CGM, (3) back calculation and (4) restraints modification was repeated iteratively until structures consistent with the experimental data could be obtained.

The structure was calculated using the DG algorithm HYGEOM^{TM}, and 30 separate structures were generated using all constrains and random input. No further refinement by energy minimization was carried out on the output of the DG calculations. RMSD (root-mean-square distances) deviations between the NMR structures were 0.65Å for the backbone. Back-calculation was made by using GNOE calculation in order to generate the theoretical NOEs. A consecutive serial files, obtained from GNOE calculation were incorporated into HYNMR^{TM} to generate NOE back-calculation spectra which can be directly compared with experimental NOESY spectra. The resultant solution state structures of zinc-binding LHRH were determined and shown in Fig. 5.

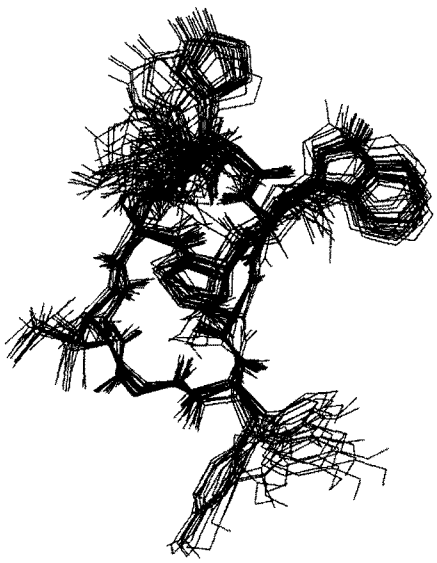

Fig. 5. Superimposed 30 restrained molecular dynamics structures of Ni-LHRH with 0.65 Å of root mean square deviation about backbone atoms.

CONCLUSIONS

Complete ^{1}H-NMR signal assignments were accomplished by utilizing 2D NMR techniques. NMR-based DG computation enabled us to determine the solution state structure of zinc binding LHRH. The final 30 structures of LHRH having 0.19~0.28Å^2 of penalty value, and 0.2~0.3Å of root mean square deviations were obtained. Nickel binding sites of LHRH are imidazole nitrogen of His[2], oxygen in peptide bond between His[2] and trp[3], and terminal NH_2 of Arg[8]. Refined structure of Ni-LHRH having 0.18~0.31Å^2 of penalty value were obtained. The backbone shape of metal complex resemble free LHRH's, like cyclic form. So far metal-LHRH studies should be focused on understanding the nature of metal-LHRH (Ni,Cu,Zn-LHRH) which may provide insight into the specific biological meanings of these transition metals. Further objectives are to establish the structural features (or coordination geometry) of the stimulated LHRH-releasing process.

Acknowledgement

Financial support from Hanyang University to H.Won is greatly acknowledged.

REFERENCES

1. Matsuo, H., Baba, Y., Nair, R. M. G., Schally, A. V., *Biochem. Biophys. Res. Commun.* **43**, 1334-1339 (1971)
2. Baba, Y., Matsuo, H., Schally, A. V., *Biochem. Biophys. Res. Commun.*, **44**, 459-463 (1971)
3. Schally, A. V., Arimura, A., Carter, W. H., Redding, T. W., Geiger, R., Kraig, W., Wissman, H., Jaeger, G., Sandow, J., *Biochem. Biophys. Res. Commun.*, **48**, 366-375 (1972)
4. Hehrman, H. R., Aten, R. F., Marcolin, Y., *Can. J. Physiol. Pharmacol.*, **67**, 954-956 (1989)
5. Hsueh, A. J., Jones, P. B. C., *Endocrine. Reviews*, **2**, 437-461 (1981)
6. Smith, R. A., Branca, A. A., Reichert Jr., L. E., *J. Biol. Chem.*, **260**, 14297-14303 (1985)

7. Ascoli, M., Segaloff, D. L., *Endocrin. Reviews.*, **11**, 27-44 (1989)
8. Shin, J., Ji, T. H., *J. Biol. Chem.*, **260**, 12828-12831 (1985)
9. van Ginkel, K. A., Loeber, J. G., *Acta Endocrinologica*, **121**, 73-82 (1989)
10. Hooper, N. M., Kenny, A. J., Turner, A. J., *Biochem. J.*, **231**, 357-361 (1985)
11. Hooper, N. M., Turner, A. J., *Bichem. J.*, **241**, 625-633 (1987)
12. Turner, A. J., *Neuropeptides and Their Peptidases*,,165-198, VCH, New York (1987)
13. Carnone, F. A., Stetler-Stevenson, M. A., May, V., Labarbera, A., Flouret, G., *Am. J. Physiol.*, **253**, E317-E321 (1987)
14. Coy, D. H., Coy, E. J., Schally, A. V., Vilchez-Martinez, J., Hirotsu, Y., Arimura, A., *Biochem. Biophys. Res. Commun.*, **57**, 335-340 (1974)
15. Monoahan, M. W., Amoss, M. S., Anderson, H. A., Vale, W., *Biochemistry*, **12**, 4616-4620 (1973)
16. Coy, D. H., Coy, E. J., Schally, A. V., *J Med. Chem.*, **16**, 1140-1143 (1973)
17. Kitajima, Y., Catt, K. J., Chen, H., *Biochem. Biophys. Res. Comm.*, **159**, 893-898 (1989)
18. Paul, P. K. C., Dauber-Osguthrope, P., Campbell, M. M., Osguthrope, D. J., *Biochem. Biophys. Res. Comm.*, **165**, 1051-1058 (1989)
19. Dutta, A. S., Gormley, J. J., McLaclan, P. F., Woodburn, J. R., *Biochem. Biophys. Res. Comm*, **159**, 1114-1120 (1989)
20. Momany, F. A., *J. Med. Chem.*, **21**, 63-68 (1978)
21. Burrows, G. H., Barnea, A., *Endocrinlogy*, **110**, 1456-1458 (1982)
22. Won, H.; Olson, K. D.; Wolfe, R. S.; Summers, M. F. *J. Am. Chem. Soc.*, **112**, 2178-2184 (1990)
23. Won, H.; Olson, K. D.; Hare, D. R.; Wolfe, R. S.; Kratky, C.; Summers, M. F. *J. Am. Chem. Soc.*, **114**, 6880-6887 (1992)
24. D. Kim, J. Rho, H. Won, *J. Kor. Mag. Reson. Soc.*, **3**, 44-51 (1999)